

Janssen effect in dynamic particulate systemsC. R. K. Windows-Yule,^{1,2} Sebastian Mühlbauer,¹ L. A. Torres Cisneros,¹ P. Nair,¹ V. Marzulli,¹ and T. Pöschel¹¹*Institute for Multiscale Simulation, Engineering of Advanced Materials,**Friedrich-Alexander Universität Erlangen-Nürnberg, Schloßplatz 4, 91054 Erlangen, Germany*²*School of Chemical Engineering, University of Birmingham, Edgbaston, Birmingham B15 2TT, United Kingdom*

(Received 4 July 2018; published 20 August 2019)

The Janssen model of stress redistribution within laterally bounded particulate assemblies is a longstanding and valuable theoretical framework, widely used in the design of industrial systems. However, the model relies on the assumption of a static packing of particles and has never been tested in a truly dynamic regime nor for a constraining system whose geometry is dynamically altered. In this paper, we explore the pressure distributions of granular beds housed within a container possessing a laterally mobile sidewall, allowing the depth, height, and cross-sectional areas of the systems studied to be dynamically altered, thus, inducing particle rearrangements and flow in the particulate system constrained thereby. We demonstrate that the systems studied can be successfully described by the Janssen model across a wide range of system expansion rates, including those for which liquidlike flow is clearly observed and propose an extension to the model allowing for an improved characterization of constrained dynamic systems.

DOI: [10.1103/PhysRevE.100.022902](https://doi.org/10.1103/PhysRevE.100.022902)**I. INTRODUCTION**

Granular materials, despite their ubiquity in, and importance to, both nature and industry [1–4], remain—as compared to classical, “molecular” materials—surprisingly poorly understood due, at least, in part, to the comparative complexity of the former, and the resultant deviations of their behaviors from the models developed to describe the latter [5,6]. A prime example of such deviation can be found in the pressure scaling behaviors of a granular material housed in a relatively tall and narrow container of uniform cross-sectional area: Whereas the pressure within a classical fluid will—under normal gravitational conditions—scale with depth as $P = \rho gz$, where ρ represents the fluid density, g represents the gravitational acceleration, and z represents the depth below the fluid’s surface. As such, the pressure felt at the base of the container will, clearly, scale linearly with the mass of fluid added. The same simple law cannot, however, be expected to hold for granular media; for these non-Newtonian materials, the pressure felt at the base of the system tends exponentially towards a finite upper limit as more material is added—i.e., there exists a point beyond which, in effect, the addition of more mass to the container will no longer be felt at the base! This rather striking observation, known as the “Janssen effect” was explained by its eponymous discoverer as a shielding effect whereby frictional contacts between grains and the system’s sidewalls act to redirect pressure towards said walls and (hence) away from the system’s base [7,8].

The theoretical model derived by Janssen to explain these effects is still widely and routinely used in industry, most notably in the design of hoppers and silos where it represents an industry-standard calculation [9–13].

A. Janssen theory

The Janssen model [7,8] predicts that, for a static granular assembly housed within an arbitrary solid-walled container,

the weight of particles within the system will be balanced by variations in the vertical component of the stress tensor σ_{zz} and frictional forces exerted by the system’s walls. As such, the stress transmitted to the base of the system ($z = 0$) can be determined as [14]

$$\sigma_{zz}^{\text{base}} = \rho \eta g \lambda (1 - e^{-H/\lambda}). \quad (1)$$

Here, H is the total height of the particle bed, ρ is the (material) density of particles, and η is the bed’s packing fraction. The coefficient λ is a characteristic length whose precise form depends on the specific geometry of the system under investigation. For the cuboidal containers explored here, λ takes the form [15]

$$\lambda = \frac{WD}{2(W + D)\kappa\mu_w}, \quad (2)$$

where W and D , respectively, are the width and the depth of the system (i.e., its extent in the Cartesian x and y coordinates—see Fig. 1), μ_w is the wall’s Coulomb friction coefficient and the Janssen coefficient κ characterizes the transmission of vertical to horizontal stresses. The coefficient κ is typically taken as a constant fitting parameter.

B. Prior work

There exists a considerable volume of scientific research relating to the Janssen effect under various different conditions [7,8,14–21]. Perhaps of the most direct relevance to the current work is the 2003 study of Bertho *et al.* [14], which demonstrated that the Janssen model can be generalized to the case in which the walls of the container exhibit motion relative to the (static) granular packing within. Their experiments involved a packing of particles contained within a hollow cylindrical tube, the tube being translated upward at a constant velocity, and the apparent mass of the particles measured. Janssen theory was observed to hold across a range

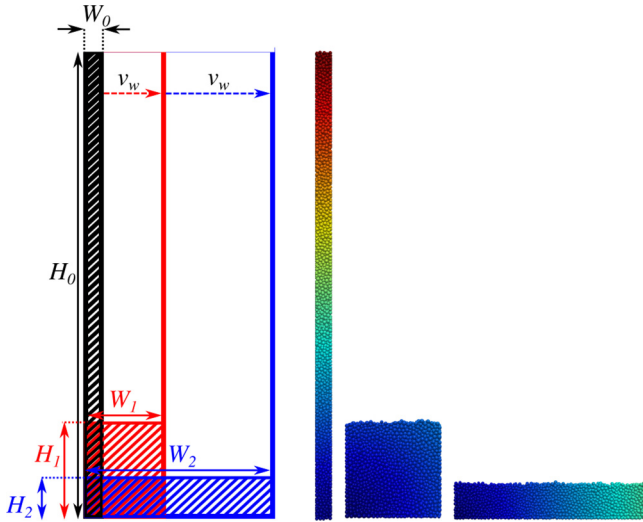


FIG. 1. Schematic providing a simplified depiction of the variation in height (H) and width (W) of the studied granular bed (hatched region) as the bounding wall moves outward in the horizontal direction, shown alongside simulated systems of equivalent width and height. The depth (D) of the system lies in the horizontal (y) direction perpendicular to the page.

of relative velocities up to the order of 1 cm/s for which the rearrangement of particles is minimized (i.e., the packing may be considered effectively static). Later work by Bratberg *et al.* [22] involved similar experiments exploring the limit of narrow granular columns, utilizing experimental cylindrical systems with widths between 1.9 and 3.5 particle diameters. Although the exponential decay of the Janssen model could be successfully fitted to the acquired data, even in these extreme cases, the expected diameter dependence of the model was *not* observed to hold.

The case of vertically moving sidewalls is also explored in simulation by Landry and Grest [23] with a focus on cases in which significant particle rearrangement *is* observed. The paper compares the stress distributions of a simple poured granular packing to one in which the particle distribution has been altered through motion of the system’s side walls, demonstrating that the Janssen model is only fully accurate if and when friction within the system is significantly “activated” (i.e., when a suitably large number of particle-particle and particle-wall contacts reach the Coulomb criterion). However, in this paper, stresses are only measured when the bed has been allowed to come to rest.

Further exploration of the importance of the fully mobilized friction condition is carried out in the simulation-based work of Vivanco *et al.* [24] who, rather than applying a simple monodirectional upward or downward translation of the container’s walls, drive friction mobilization instead via a cyclic vertical displacement of the system’s containing walls. This cyclic motion acts to repeatedly mobilize and then inversely mobilize friction, thus, acting to modify the stress profiles observed. For relatively shallow beds, the Janssen model is found to hold for all phases of the cyclic motion, although the sign of the exponent in Eq. (1) is reversed for the case of inversely mobilized friction. For taller systems, the distribution of stresses is more complex with coexisting re-

gions of full, partial, and/or inverse friction mobilization; the authors propose a generalization of the Janssen model capable of describing the behaviors of these more complicated cases also. Once again, data are acquired in the absence of any significant particle rearrangement as the systems explored remain jammed [25,26] throughout the majority of the simulations.

Most recently, Blanco-Rodríguez and Pérez-Ángel [27] investigated the influence of various key parameters—namely, the frictional coefficient, particle size, bed width, and particle polydispersity—on the stress distributions within a two-dimensional system. Notably, it was found that as the width of their system was increased relative to the particle diameter—even at a constant aspect ratio H/W —the Janssen model becomes less relevant. Specifically, their results suggest that the system approaches hydrostaticity (i.e., the Janssen model breaks down) for a ratio $\frac{R_{\text{ave}}}{L} \lesssim 0.008$, where R_{ave} is the mean particle diameter.

C. Aims and motivation

Despite the significant research effort discussed above, to the authors’ knowledge, the Janssen model has thus far been applied only to static packings. Even in the case of Bertho *et al.* [14] where there exists relative motion between a particulate system and its housing container, the granulate itself remains static and solidlike, and the container’s cross-sectional area remains constant. As such, there remains a significant open question regarding the applicability of Janssen’s theory to dynamic systems where particles exhibit rearrangements and relative motion. If the Janssen model—or a variant thereof—can be shown to hold also for dynamic particulate systems, this may prove a significant aid to the safe and precise design of a variety of systems, such as the tall narrow rotating drums used widely in the Australian mining industry, compaction systems in the waste, pharmaceutical, and nuclear industries, and the numerous systems in a variety of industries involving the transport of particles through vertical pipes [28–30].

Perhaps one of the most interesting contemporary applications of a dynamic Janssen theory is in the design of future lunar bases [31] where beds of lunar regolith housed in containers with laterally mobile bounding walls may be used as shielding to mitigate the destructive effects of micrometeorite impacts. It is this particular geometry which we explore in the present paper—although the theoretical derivation presented may be easily adapted to other dynamic systems. Specifically, in this paper, we explore—via numerical simulation—the variation in the force exerted upon the base of a system housing a granular material of fixed mass and particle number as the width—and, hence, vertical cross-sectional area—of said system is altered by the horizontal displacement of a single bounding wall. Our results provide a demonstration that the Janssen model may be successfully extended to the case of dynamic granular systems.

II. SIMULATIONS

A. Simulation model

Our numerical simulations are produced using the MERCURYDPM discrete element method software package [32–35],

utilizing a spring-dashpot model [36,37] with linear elastic and dissipative contributions for the determination of both normal and tangential forces.

The normal and tangential forces acting between a pair of particles i and j are given, respectively, as [37,38]

$$f_{ij}^n = k^n \delta_{ij}^n \hat{\mathbf{n}}_{ij} - \zeta^n \mathbf{v}_{ij}^n, \quad (3)$$

and

$$f_{ij}^t = -k^t \delta_{ij}^t - \zeta^t \mathbf{v}_{ij}^t. \quad (4)$$

In the above, the parameters \mathbf{v}_{ij}^n and \mathbf{v}_{ij}^t represent, respectively, the normal and tangential components of the relative velocity between particles i and j with δ_{ij}^t as the *tangential displacement* (for further details, see Ref. [39]). The normal spring and damping constants, k^n and ζ^n , respectively, are determined as

$$k^n = m_{ij} \left[\left(\frac{\pi}{t_c} \right)^2 - \left(\frac{\ln \varepsilon}{t_c} \right)^2 \right], \quad (5)$$

and

$$\zeta^n = -2m_{ij} \left(\frac{\ln \varepsilon}{t_c} \right) \quad (6)$$

based on a given restitution coefficient ε and contact time t_c [40]. For the current paper, we implement a contact time of $t_c = 1 \times 10^{-6}$ s. The reduced mass m_{ij} for a given pair of colliding particles is computed as

$$m_{ij} = \frac{m_i m_j}{m_i + m_j}. \quad (7)$$

The *tangential* spring and damping constants are determined from their normal counterparts as $k^t = \frac{2}{7} k^n$ and $\zeta^t = \zeta^n$, respectively.

A Coulomb-type friction law is implemented with a static yield criterion applied in such a manner as to truncate the tangential force f_{ij}^t , acting between two contacting particles i and j according to the inequality $f_{ij}^t \leq \mu f_{ij}^n$, where f_{ij}^n is the normal force acting between the aforementioned particles and μ is the relevant frictional coefficient. In the current paper, the frictional coefficient is assigned a value of $\mu = 0.5$, and the restitution coefficient, which determines energy loss due to collisional dissipation, is assigned a value of $\varepsilon = 0.8$. The above-described model has previously been shown to successfully recreate the behaviors of dense granular flows, such as those explored here [41,42]. Stresses within the system are determined using the coarse-graining [43] methodology developed by Weinhart *et al.*, full details of which may be found in Ref. [44].

B. Simulated system

We simulate an open system bounded by five smooth frictional walls, comprising a horizontal base plate and four vertical sidewalls. In its initial state, the system possesses a width and depth of $W_0 = D_0 = 0.025$ m and a height of $H_0 = 0.75$ m. The system is filled, via pouring, with a number $N = 3183$ of 5 mm (mean) diameter spherical particles to create a randomly packed bed which fills the system (see Fig. 1). The diameters of the simulated particles are varied uniformly by $\pm 5\%$ so as to prevent the unrealistic crystallization of particles and, hence, nonrepresentative behavior, which can occur if

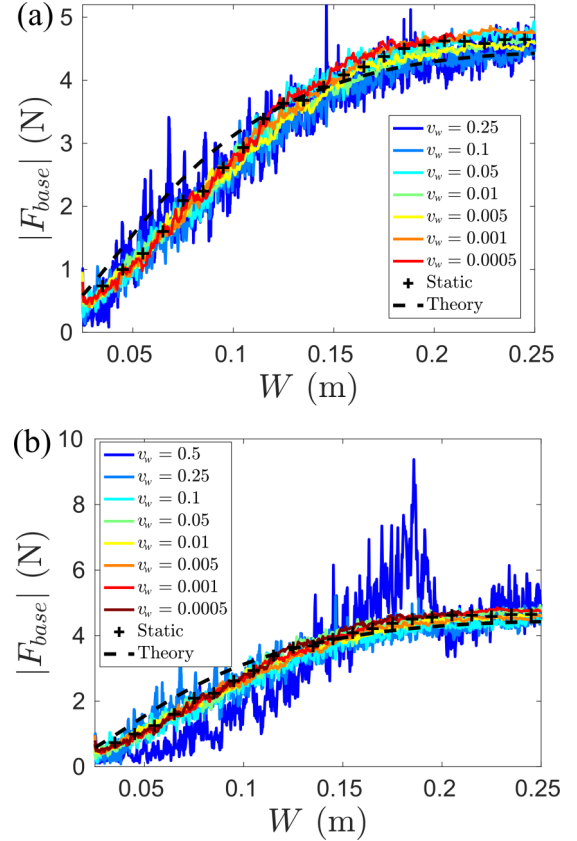


FIG. 2. Variation with system width W of the total force exerted on the base of the housing container for the case of a wall moving at an externally imposed fixed velocity v_w (continuous lines) and for a series of equivalent static systems of differing fixed width (symbols). Plotted also (dashed line) is theoretical fit following the conventional Janssen model [Eqs. (1) and (2)]. Data are shown for various values of v_w , given in the legends provided in units of meters per second; image (a) omits data for $v_p = 0.5$ m/s such that the trend followed by the lower-velocity systems may be more clearly observed.

particles are modeled with zero polydispersity. All particles are assigned an equal material density of $\rho = 2500$ kg m $^{-3}$. The system is exposed to a gravitational acceleration of $g = 9.81$ ms $^{-2}$ in the negative vertical direction.

III. RESULTS

A. Conventional Janssen scaling

In Fig. 2, we show the variation with system width of the total force (i.e., the effective particle weight) felt by the base of the container for a variety of different outward wall velocities v_w . First notable from this figure is the fact that, despite the constant mass of material (and, hence, fixed “true” weight), the *effective* weight F_{base} , felt by the base varies by approximately an order of magnitude as the bed’s width W increases and its height H correspondingly decreases. This observation, although not unexpected, provides a clear demonstration of the considerable influence of the Janssen effect in our system.

A second, and perhaps more surprising, observation is that for dynamic systems with wall velocities ranging from one tenth of a particle diameter per second up to the significant rate

of 50 particle diameters per second, the observed $F_{\text{base}}-W$ relations all approximately collapse onto a single master curve—although higher-velocity data sets show stronger fluctuations.

Finally, and perhaps most significantly for the aims of this paper, we find that the trend is followed also for *static* systems of differing (fixed) widths. In other words, we may safely assume that—in our present system—for $v_w \lesssim 50 d/s$, for any fixed point in time, the Janssen model may be safely expected to hold.

For higher-still velocities, agreement with the Janssen model is found to break down (see Fig. 2, lower) as the wall velocity becomes such that complete detachment between bed and boundary occurs. The strong deviations from the predicted form for the case of $v_w = 0.5$ can be relatively easily explained: during the wall's initial rapid motion, the bed becomes detached from the wall, and particles cascade downwards to fill the void created. As a fraction of the cascading, particles will enter freefall, their weight will not be propagated through the system and, hence, not felt by the base, leading to the initial reduction in F_{base} as compared to the other data sets. As the system expands further ($W \sim 0.18$ m), the freefalling particles recollide with the bed and/or base of the system, creating an impact force not experienced by the lower- v_w systems and, thus, a relatively increased F_{base} .

In short, our results strongly suggest that the Janssen model can be expected to be applicable for any system in which continuous contact between particles (i.e., an absence of wall detachment or particle freefall) may be assumed.

B. A dynamic Janssen model

Although the Janssen model may indeed be expected to provide a good description of our system at any given point in time—i.e., any given single width—when we attempt to fit the model to our dynamic data, the agreement is clearly imperfect (see Fig. 2, dashed line). In particular, we observe a systematic overestimation of F_{base} for small W and an underestimation for larger W . This disagreement between theory and simulation can most likely be explained by the dubious assumption of a constant Janssen coefficient κ . Although such an assumption is reasonable for the fixed-width containers explored in prior works, it cannot necessarily be expected to hold in our beds where the width (and hence), height, and cross-sectional areas vary significantly with time. In other words, we must consider instead a “dynamic Janssen coefficient” $\tilde{\kappa} = \kappa(W, H)$. It follows from the Janssen model that κ may be determined from the ratio of horizontal and vertical principal stresses within the system as detailed in Ref. [8], i.e.,

$$\kappa = \mu \frac{\sigma_{\text{wall}}}{\sigma_{\text{base}}} = \mu \frac{F_{\text{wall}} A_{\text{base}}}{F_{\text{base}} A_{\text{wall}}}, \quad (8)$$

where A_{wall} and A_{base} are the relevant particle-wall contact areas upon which the horizontal and vertical forces, respectively, are exerted. We begin by assuming quasistatic motion, i.e., the original static Janssen model is valid for any given value of W , meaning that the general form of σ_{base} may be calculated from Eq. (1). The validity of this assumption is supported by the fact that—as demonstrated in Fig. 2—equivalent dynamic and static systems seemingly obey the same force-width relation.

In order to determine a relation between the horizontal and the vertical wall-particle contact areas A_{wall} and A_{base} , we begin by assuming that the bed occupies a constant total volume $V_0 = W_0 \times D_0 \times H_0$ (where W_0 , H_0 , and D_0 are constants representing the initial dimensions of the bed as depicted in Fig. 1). We consider first A_{base} , which corresponds simply to the area of the base of the system. As our system maintains a fixed depth of $D = D_0$, the width-dependent base area can be written as

$$A_{\text{base}}(W) = D_0 W. \quad (9)$$

Second, we consider A_{wall} , which corresponds to the contact area of the bed with the four bounding lateral walls of the system. The two static bounding walls in the y direction will maintain a constant contact area, whereas the two walls bounding the system in the direction of motion (i.e., the x direction) will see a decrease in area as $\frac{1}{W}$. As such, the total horizontal contact area at a given system width W can be calculated as

$$A_{\text{wall}} = 2(W_0 H_0 + D_0 H), \quad (10)$$

where $H = H(W) = \frac{H_0 W_0}{W}$, i.e.,

$$A_{\text{wall}}(W) = 2W_0 H_0 \left(1 + \frac{D_0}{W} \right). \quad (11)$$

Equation (1) may be trivially expanded to give the total force acting on the base of our system as

$$F_{\text{base}} = A_{\text{base}} \sigma_{\text{base}} = D_0 W \rho \eta g \lambda (1 - e^{-H/\lambda}). \quad (12)$$

Knowing that—as the total mass M_p of particles remains constant—the total weight of the particles within the system is given by

$$F_g = M_p g = \rho \eta g W_0 D_0 H_0, \quad (13)$$

and that the difference between this total force and the force felt by the bed must be borne by the system sidewalls, the *tangential* force exerted by the walls can, therefore, be given as

$$F_{\text{wall}}^t = F_g - F_{\text{base}} = \rho \eta g D_0 [W_0 H_0 - W \lambda (1 - e^{-H/\lambda})]. \quad (14)$$

Assuming, as per the conventional Janssen model, fully mobilized Coulombic friction, the *normal* wall force can then be given as

$$F_{\text{wall}} = \frac{\rho \eta g D_0}{\mu} [W_0 H_0 - W \lambda (1 - e^{-H/\lambda})]. \quad (15)$$

Combining Eqs. (1), (8), (11), and (15), we obtain an expression for the dynamic Janssen coefficient,

$$\begin{aligned} \tilde{\kappa} &= \mu \frac{\sigma_{\text{wall}}}{\sigma_{\text{base}}} = \mu \frac{F_{\text{wall}}}{A_{\text{wall}} \sigma_{\text{base}}} \\ &= \frac{\rho \eta g D_0 [W_0 H_0 - W \lambda (1 - e^{-H/\lambda})]}{2W_0 H_0 \left(1 + \frac{D_0}{W} \right) \rho \eta g \lambda (1 - e^{-H/\lambda})}, \end{aligned} \quad (16)$$

which can be simplified to give

$$\tilde{\kappa} = \frac{W D_0}{2(W + D_0)} \left[\frac{1}{\tilde{\lambda} (1 - e^{-H/\tilde{\lambda}})} - \frac{W}{W_0 H_0} \right], \quad (17)$$

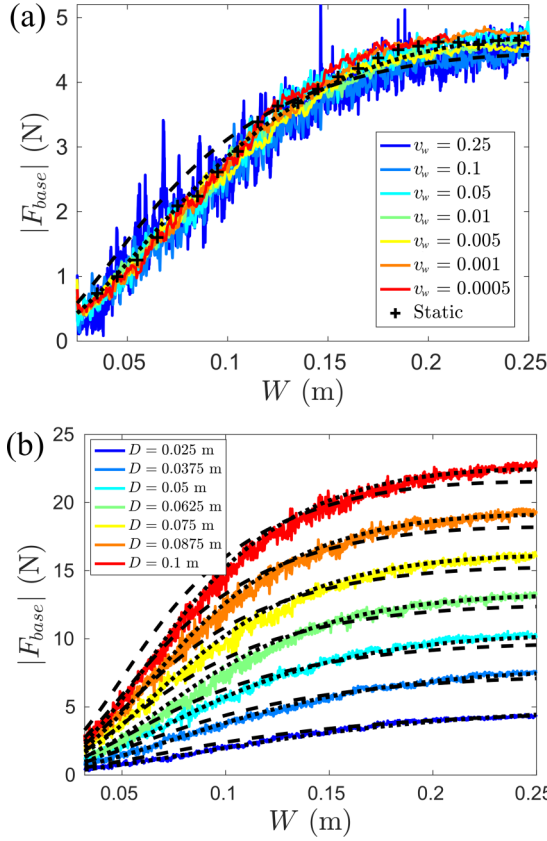


FIG. 3. (a) Variation of the effective weight felt by the system base F_{base} with the system width W for the varying-velocity data originally shown in Fig. 2. (b) Variation of F_{base} with W for a variety of different horizontal system depths D_0 at fixed initial height $H_0 = 0.75$ m, thereby providing also a variation in the true weight M_{pg} of the system. All data shown in this panel are conducted at a fixed wall velocity of $v_w = 0.01$ m/s $= 2d$. In both cases, fits corresponding to the classical (constant κ) modified (dynamic $\tilde{\kappa}$) Janssen models are represented by dashed and dotted lines, respectively.

where λ retains a dependence on a constant “static κ ” which, as in the original Janssen model, may be used as a fitting parameter.

In Fig. 3, we show a series of F_{wall} - W curves for beds possessing not only a range of expansion velocities, but also a range of horizontal bed depths $D_0 \in [0.025, 0.1]$ and, hence, varying total masses M_p , each fitted by Eq. (1) with both fixed [Eq. (2), dashed lines] and dynamic [Eq. (17), dotted lines] Janssen coefficients; in both cases, a single value of the static Janssen coefficient $\kappa = 0.225$ (corresponding to a “static decay length” $\lambda = 0.06$ m) is utilized for *all* simulated systems. Whereas even the unaltered Janssen model can be seen to provide a reasonable description of the systems’ behavior, the extended model provides a superior fit in all cases, despite the significant variation in both the bed’s horizontal depth and the mass. It is valuable to note that the model is, for all tested cases, found to produce strong agreement for all W - H combinations for which the system walls can be expected to bear any appreciable fraction of the system’s weight—in other words, our results imply the modified model to be valid as long as the Janssen effect is, in fact, present.

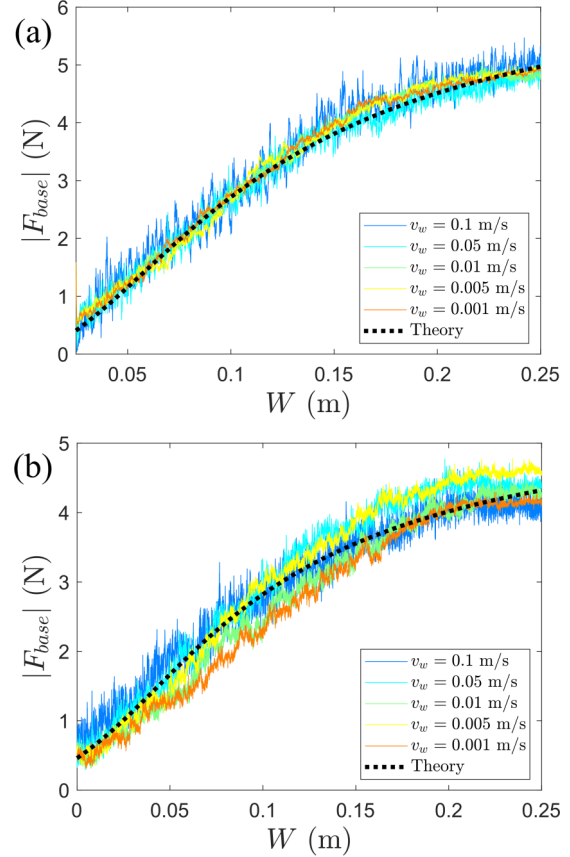


FIG. 4. Variation of effective weight F_{base} with system width for a fixed bed depth of $D_0 = 0.025$ m and initial bed height of $H_0 = 0.75$ m and particle-particle frictional coefficient $\mu = 0.5$. Data are shown for wall-friction coefficients $\mu_w = 0.25$ [panel (a)] and $\mu_w = 1.0$ [panel (b)]. In both cases, the black dotted line represents a fit corresponding to the modified Janssen model.

In Fig. 4, we show data for a system in which the particle-particle friction coefficient (μ_p) remains constant at a value $\mu_p = 0.5$, whereas the particle-wall restitution coefficient takes on values of 0.25 ($\mu_w = \frac{\mu_p}{2}$) and 1 ($\mu_w = 2\mu_p$). In both cases, we see that the modified Janssen equation continues to provide a good description of the systems’ behaviors across a range of wall velocities and frictional coefficients even for the case in which $\mu_w \neq \mu_p$.

C. The “free wall” case

Thus far, we have considered the case in which the particle transport within our system is driven by an externally imposed prescribed motion. Whereas this situation is typical to a majority of industrial applications, we consider now the case of a mechanically unstable free wall, whose motion is driven by the horizontal pressure exerted by the bed constrained thereby—the situation more relevant to the lunar-base-shielding application [31] discussed in Sec. IC. To test this case, we simulate a bed of particles identical to that discussed in previous sections, bounded in the lateral directions by three rigid fixed walls and one free wall of mass M_w whose motion is determined by the balance between outward pressure from the particle bed and the frictional force

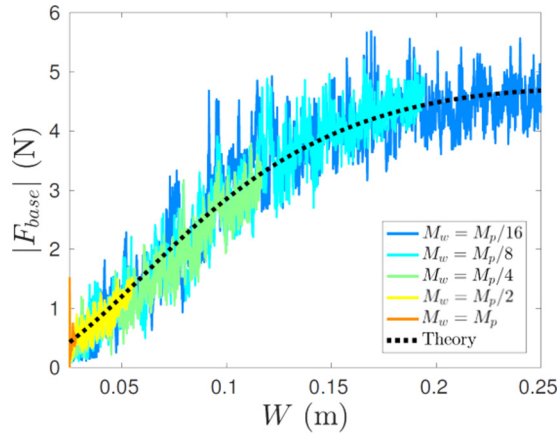


FIG. 5. Variation of F_{base} with system width for the case of a free bounding lateral wall for walls of varying mass M_w . The dotted line corresponds to the modified Janssen model utilizing the same $\tilde{\kappa}$ as in Fig. 3. It is interesting to note that the observed force-width relation is seemingly independent of the wall bounding wall mass for the range of M_w explored.

between the wall and the base of the system. For simplicity and ease of interpretation, the free wall is constrained to remain vertical and possess a constant frictional coefficient $\mu_w = \mu_p = 0.5$. The system's initial conditions match those described in Sec. II B. In Fig. 5, we plot a curve corresponding to our dynamical Janssen model using the same $\tilde{\kappa}$ as for Fig. 3, alongside simulated force vs width data for simulations using free walls of mass $M_w \in [\frac{1}{16}M_p, M_p]$. Although the simulated curves obtained are significantly noisier than those obtained via externally imposed wall motion, curves for a variety of wall masses are all observed to follow the same broad trend predicted by the modified Janssen model. Note that the length of the various curves is limited by the equilibrium point of the wall (i.e., how far a wall of given mass can be expected to move before the outward force exerted by the bed is balanced by the opposing frictional force).

D. Limits of validity

It is finally valuable to consider the relevant timescales which govern the appropriateness and quality of the predictions provided by our modified Janssen model and, hence, establish the limits of its applicability—as well as providing insight into the origin of the surprisingly wide range of velocities across which said model is seemingly valid. In any granular system, we may consider a value of $\tau_g = \sqrt{\frac{2d}{g}}$, corresponding to the time required for an initially static

particle to fall through a distance equal to its own diameter as a timescale relevant to said system's dynamical behaviors. The behavior of our current system of interest can be predicted by comparing a second natural timescale $\tau_w = \frac{d}{v_w}$, the time required for the moving wall to travel one particle diameter, to the previously defined timescale. For the case of $\tau_w \gg \tau_g$, the system can be assumed to behave quasistatically, meaning that we may expect our system to be well described by the modified Janssen model. For our present system, the aforementioned condition implies that our model may be expected to hold, to a reasonable extent, for wall velocities $v_w \lesssim 0.15$, a prediction borne out by the data presented in Figs. 2 and 3. Notable also from these figures is that as the relevant timescale approaches and begins to exceed the granular timescale τ_g , the fluctuations about the predicted F_{base} values begin to increase as the separation of the two relevant timescales becomes diminished, with agreement breaking down entirely only as the timescales significantly diverge at large v_w .

IV. CONCLUSIONS

In this paper, we have detailed a test of the validity of the Janssen pressure-scaling model for dynamic granular systems possessing a nonconstant characteristic length. In doing so, we have demonstrated that the underlying physics of the system may indeed be successfully described by the basic principles of the Janssen model, even at significant bed-expansion velocities. Indeed, our results strongly imply that the Janssen model can be expected to be held for all cases in which continual contact between neighboring particles—and, where relevant, the system walls—can be expected.

Furthermore, we have provided an extension to the original (static) Janssen model for the case of a dynamically expanding system and shown this model to accurately predict the behavior of such systems across a range of expansion velocities, system extensions, system widths, particle-wall friction values, and bed masses. Furthermore, we have shown the modified theory to hold both for the case of externally imposed wall motion as well as for that of a free bounding wall.

The ability to better understand and predict the behaviors of laterally constrained dynamic systems—for example, the high-aspect-ratio tumblers used in the mining industry or numerous applications involving pipe flow—may prove highly valuable to future research, both academic and industrial. In particular, the applicability of our model to systems bounded by free walls will directly benefit contemporary research concerning impact shielding for lunar structures.

[1] P.-G. de Gennes, *Rev. Mod. Phys.* **71**, S374 (1999).
 [2] F. J. Muzzio, T. Shinbrot, and B. J. Glasser, *Powder Technol.* **124**, 1 (2002).
 [3] P. Tegzes, T. Vicsek, and P. Schiffer, *Phys. Rev. Lett.* **89**, 094301 (2002).
 [4] E. B. Pitman, C. C. Nichita, A. Patra, A. Bauer, M. Sheridan, and M. Bursik, *Phys. Fluids* **15**, 3638 (2003).

[5] H. M. Jaeger and S. R. Nagel, *Science* **255**, 1523 (1992).
 [6] H. M. Jaeger, S. R. Nagel, and R. P. Behringer, *Rev. Mod. Phys.* **68**, 1259 (1996).
 [7] H. Janssen, *Zeitschr. d. Vereines deutscher Ingenieure* **39**, 1045 (1895).
 [8] M. Sperl, *Granular Matter* **8**, 59 (2006).
 [9] C. V. Schwab, I. J. Ross, G. M. White, and D. G. Colliver, *Trans. ASAE* **37**, 1613 (1994).

- [10] S. Thompson, N. Galili, and R. Williams, *Trans. ASAE* **39**, 1093 (1996).
- [11] D. Schulze, <http://www.dietmar-schulze.de/spannepr.html>
- [12] D. Schulze, *Powders and Bulk Solids: Behavior, Characterization, Storage and Flow* (Springer, Berlin/Heidelberg, 2008), p. 291.
- [13] D. Schulze, *Production, Handling and Characterization of Particulate Materials* (Springer, Berlin, 2016), pp. 425–478.
- [14] Y. Bertho, F. Giorgiutti-Dauphiné, and J.-P. Hulin, *Phys. Rev. Lett.* **90**, 144301 (2003).
- [15] J. W. Landry, G. S. Grest, and S. J. Plimpton, *Powder Technol.* **139**, 233 (2004).
- [16] E. Kolb, T. Mazozi, E. Clément, and J. Duran, *Eur. Phys. J. B* **8**, 483 (1999).
- [17] G. Ovarlez, C. Fond, and E. Clément, *Phys. Rev. E* **67**, 060302(R) (2003).
- [18] J. F. Wambaugh, R. R. Hartley, and R. P. Behringer, *Eur. Phys. J. E* **32**, 135 (2010).
- [19] L. Vanel and E. Clément, *Eur. Phys. J. B* **11**, 525 (1999).
- [20] J. Ai, Particle scale and bulk scale investigation of granular piles and silos, Ph.D. thesis, University of Edinburgh, 2010.
- [21] R. Butterfield, *International Journal of Rock Mechanics and Mining Sciences & Geomechanics Abstracts* (Elsevier, Amsterdam, 1969), Vol. 6, pp. 227–238.
- [22] I. Bratberg, K. Måløy, and A. Hansen, *Eur. Phys. J. E* **18**, 245 (2005).
- [23] J. W. Landry and G. S. Grest, *Phys. Rev. E* **69**, 031303 (2004).
- [24] F. Vivanco, J. Mercado, F. Santibáñez, and F. Melo, *Phys. Rev. E* **94**, 022906 (2016).
- [25] A. J. Liu and S. R. Nagel, *Nature (London)* **396**, 21 (1998).
- [26] C. Song, P. Wang, and H. A. Makse, *Nature (London)* **453**, 629 (2008).
- [27] R. Blanco-Rodríguez and G. Pérez-Ángel, *Phys. Rev. E* **97**, 012903 (2018).
- [28] J. O'Rourke and M. Feldberg, "Vertical waste compacting apparatus", U.S. Patent No. 4,073,229 (14 February 1978).
- [29] C. Ran, J. J. K. Daemen, M. D. Schuhen, and F. D. Hansen, *Int. J. Rock Mech. Min. Sci.* **34**, 253.e1 (1997).
- [30] Y. Bertho, F. Giorgiutti-Dauphiné, and J.-P. Hulin, *Phys. Fluids* **15**, 3358 (2003).
- [31] F. Cafaro, E. Miticocchio, and V. Marzulli, *Stud. Geotech. Mech.* **40**, 133 (2018).
- [32] A. R. Thornton, T. Weinhart, S. Luding, and O. Bokhove, *Int. J. Mod. Phys. C* **23**, 1240014 (2012).
- [33] A. R. Thornton, T. Weinhart, V. Ogarko, and S. Luding, *Comput. Methods Mater. Sci.* **13**, 197 (2013).
- [34] A. R. Thornton, D. Krijgsman, A. te Voortwis, V. Ogarko, S. Luding, R. Fransen, S. Gonzalez, O. Bokhove, O. Imole, and T. Weinhart, *DEM 6: Proceedings of the 6th International Conference on Discrete Element Methods and Related Techniques, Golden, CO, 2013* (Colorado School of Mines, Golden, CO, 2013), p. 393.
- [35] T. Weinhart, D. Tunuguntla, M. van Schrojenstein-Lantman, A. van der Horn, I. Denissen, C. Windows-Yule, A. de Jong, and A. Thornton, in *Proceedings of the 7th International Conference on Discrete Element Methods*, edited by X. Li, Y. Feng, and G. Mustoe, Springer Proceedings in Physics Vol. 188 (Springer, Singapore, 2016), pp. 1353–1360.
- [36] P. A. Cundall and O. D. Strack, *Geotechnique* **29**, 47 (1979).
- [37] S. Luding, *European J. Environ. Civil Eng.* **12**, 785 (2008).
- [38] O. R. Walton, *Int. J. Eng. Sci.* **22**, 1097 (1984).
- [39] T. Weinhart, A. R. Thornton, S. Luding, and O. Bokhove, *Granular Matter* **14**, 531 (2012).
- [40] S. Luding and S. McNamara, *Granular Matter* **1**, 113 (1998).
- [41] D. R. Tunuguntla, O. Bokhove, and A. R. Thornton, *J. Fluid Mech.* **749**, 99 (2014).
- [42] D. R. Tunuguntla, T. Weinhart, and A. R. Thornton, *Comput. Part. Mech.* **4**, 387 (2017).
- [43] I. Goldhirsch, *Granular Matter* **12**, 239 (2010).
- [44] T. Weinhart, A. R. Thornton, S. Luding, and O. Bokhove, *Granular Matter* **14**, 289 (2012).